arXiv:0710.1897v2 [astro-ph] 2 Aug 2008

GRAVITATIONAL-WAVE ASTRONOMY WITH INSPIRAL SIGNALS OF SPINNING COMPACT-OBJECT BINARIES

M. V. VAN DER SLUYS[1], C. RÖVER[2,3], A. STROEER[1,4], V. RAYMOND[1], I. MANDEL[1],
N. CHRISTENSEN[5], V. KALOGERA[1], R. MEYER[2], A. VECCHIO[1,4]
Draft version August 2, 2008

ABSTRACT

Inspiral signals from binary compact objects (black holes and neutron stars) are primary targets of the on-going searches by ground-based gravitational-wave interferometers (LIGO, Virgo, GEO-600 and TAMA-300). We present parameter-estimation simulations for inspirals of black-hole–neutron-star binaries using Markov-chain Monte-Carlo methods. For the first time, we have both estimated the parameters of a binary inspiral source with a spinning component and determined the accuracy of the parameter estimation, for simulated observations with ground-based gravitational-wave detectors. We demonstrate that we can obtain the distance, sky position, and binary orientation at a higher accuracy than previously suggested in the literature. For an observation of an inspiral with sufficient spin and two or three detectors we find an accuracy in the determination of the sky position of typically a few tens of square degrees.

Subject headings: Binaries: close, Gamma rays: bursts, Gravitational waves, Relativity

1. INTRODUCTION

Binary systems with compact objects — neutron stars (NS) and black holes (BH) — in the mass range $\sim 1 M_\odot - 100 M_\odot$ are among the most likely sources of gravitational waves (GWs) for ground-based laser interferometers currently in operation (Cutler & Thorne, 2002): LIGO (Barish & Weiss 1999), Virgo (Arcese et al. 2004), GEO-600 (Willke et al. 2004) and TAMA-300 (Takahashi et al. 2004). Merger-rate estimates are quite uncertain and for BH-NS binaries current detection-rate estimates reach as high as $0.1 \, \mathrm{yr}^{-1}$ (*e.g.* O'Shaughnessy et al. 2008) for first-generation instruments. Upgrades to Enhanced LIGO/Virgo (2008–2009) and Advanced LIGO/Virgo (2011–2014) are expected to increase detection rates by factors of about ~ 8 and 10^3, respectively.

The measurement of astrophysical source properties holds major promise for improving our physical understanding and requires reliable methods for parameter estimation. This is a challenging problem because of the large number of parameters (> 10) and the presence of strong correlations among them, leading to a highly-structured parameter space. In the case of high mass ratio binaries (*e.g.* BH-NS), these issues are amplified for significant spin magnitudes and large spin misalignments (Apostolatos et al. 1994; Grandclément et al. 2003; Buonanno et al. 2003). However, the presence of spins benefits parameter estimation through the signal modulations, although still presenting us with a considerable computational challenge. This has been highlighted in the context of LISA observations (see Vecchio 2004; Lang & Hughes 2006) but no study has been devoted so far to ground-based observations.

In this *Letter* we examine for the first time the potential for parameter estimation of spinning binary inspirals with ground-based interferometers, including twelve physical parameters. Earlier studies (*e.g.* Cutler & Flanagan 1994, Poisson & Will 1995, Van den Broeck & Sengupta 2007) have estimated the theoretical accuracy with which some of these parameters should be measured, without determining

the parameters themselves. Also, (Röver et al. 2006, 2007) have explored parameter estimation for non-spinning binaries. We focus on BH-NS binaries where spin effects are strongest (Apostolatos et al. 1994), while at the same time we are justified to ignore the NS spin. We employ a newly developed Markov-chain Monte-Carlo (MCMC) algorithm (van der Sluys et al. 2008) applied on spinning inspiral signals injected into synthetic ground-based noise and we derive posterior probability-density functions (PDFs) of all twelve signal parameters. We show that although sky position is degenerate when using two detectors, we can still determine the mass and spin parameters to reasonable accuracy. With three detectors, the sky position and binary orientation can be fully resolved. We show that our accuracies are good enough to associate an inspiral event with an electromagnetic detection, such as a short gamma-ray burst (*e.g.* Nakar 2007).

2. SIGNAL AND OBSERVABLES

In this *Letter* we concentrate on the signal produced during the inspiral phase of two compact objects of masses $M_{1,2}$ in circular orbit. We focus on a fiducial BH-NS binary system with $M_1 = 10 M_\odot$ and $M_2 = 1.4 M_\odot$, so that we can ignore the NS spin. The BH spin **S** couples to the orbital angular momentum, leading to amplitude and phase modulation of the observed radiation due to the precession of the orbital plane during the observation. Here we model GWs by post-Newtonian (pN) waveforms at $^{1.5}$-pN order in phase and Newtonian amplitude. We adopt the *simple-precession* limit (Eqs. 51, 52, 59 & 63 in Apostolatos et al. 1994), appropriate for the single-spin system considered here. For simplicity (to speed up the waveform calculation), we ignore the *Thomas-precession phase* (Apostolatos et al. 1994). In this simple-precession approximation, the orbital angular momentum **L** and spin **S** precess with the *same* angular frequency around a fixed direction $\hat{\mathbf{J}}_0 \approx \hat{\mathbf{J}}$, where $\mathbf{J} = \mathbf{L} + \mathbf{S}$. During the inspiral phase the spin misalignment $\theta_{\mathrm{SL}} \equiv \arccos(\hat{\mathbf{S}} \cdot \hat{\mathbf{L}})$ and $S = |\mathbf{S}|$ are constant. These approximated waveforms retain (at the leading order) all the salient qualitative features introduced by the spins, while allowing us to compute the waveforms analytically, at great computational speed. While this approach is justified for exploration of GW astronomy and development of parameter-estimation algorithms, more accurate

[1] Physics & Astronomy, Northwestern U., Evanston IL, USA
[2] Statistics, U. of Auckland, Auckland, New Zealand
[3] Max-Planck-Institut für Gravitationsphysik, Hannover, Germany
[4] Physics & Astronomy, U. of Birmingham, Edgbaston, Birmingham, UK
[5] Physics & Astronomy, Carleton College, Northfield MN, USA

waveforms (*e.g.* Kidder 1995; Faye et al. 2006; Blanchet et al. 2006) will be necessary for the analysis of real signals.

A circular binary inspiral with one spinning compact object is described by a 12-dimensional parameter vector $\vec{\lambda}$. With respect to a fixed geocentric coordinate system our choice of independent parameters is:

$$\vec{\lambda} = \{\mathcal{M}, \eta, \text{R.A.}, \text{Dec}, \cos\theta_{J_0}, \phi_{J_0}, \log d_L, a_{\text{spin}}, \cos\theta_{\text{SL}}, \phi_c, \alpha_c, t_c\}, \quad (1)$$

where $\mathcal{M} = \frac{(M_1 M_2)^{3/5}}{(M_1+M_2)^{1/5}}$ and $\eta = \frac{M_1 M_2}{(M_1+M_2)^2}$ are the chirp mass and symmetric mass ratio, respectively; R.A. (right ascension) and Dec (declination) identify the source position in the sky; the angles θ_{J_0} and ϕ_{J_0} (defined in the range $\theta_{J_0} \in \left[-\frac{\pi}{2}, \frac{\pi}{2}\right]$ and $\phi_{J_0} \in [0, 2\pi[$) identify the unit vector $\hat{\mathbf{J}}_0$; d_L is the luminosity distance to the source and $0 \leq a_{\text{spin}} \equiv S/M_1^2 \leq 1$ is the dimensionless spin magnitude; ϕ_c and α_c are integration constants that specify the GW phase and the location of $\mathbf{S}$ on the precession cone, respectively, at the time of coalescence t_c.

Given a network comprising n_{det} detectors, the data collected at the a–th instrument ($a = 1, \ldots, n_{\text{det}}$) is given by $x_a(t) = n_a(t) + h_a(t; \vec{\lambda})$, where $h_a(t; \vec{\lambda}) = F_{a,+}(t) h_{a,+}(t; \vec{\lambda}) + F_{a,\times}(t) h_{a,\times}(t; \vec{\lambda})$ is the GW strain at the detector (see Eqs. 2–5 in Apostolatos et al. 1994) and $n_a(t)$ is the detector noise. The astrophysical signal is given by the linear combination of the two independent polarisations $h_{a,+}(t; \vec{\lambda})$ and $h_{a,\times}(t; \vec{\lambda})$ weighted by the *time-dependent* antenna beam patterns $F_{a,+}(t)$ and $F_{a,\times}(t)$. An example of h_a for $\theta_{\text{SL}} = 20°$ and $a_{\text{spin}} = 0.1$ and 0.8 is shown in panels a–b of Fig. 1. In our analysis we model the noise in each detector as a zero-mean Gaussian, stationary random process, with one-sided noise spectral density $S_a(f)$ at the initial-LIGO design sensitivity, where f is the frequency.

3. PARAMETER ESTIMATION: METHODS AND RESULTS

The goal of our analysis is to determine the *posterior* PDF of the unknown parameter vector $\vec{\lambda}$ in Eq. (1), given the data sets x_a collected by a network of n_{det} detectors and the *prior* $p(\vec{\lambda})$ on the parameters. We use wide, flat priors (see Van der Sluys et al. 2008 for details). Bayes' theorem provides a rigorous mathematical rule to assign such a probability:

$$p(\vec{\lambda}|x_a) = \frac{p(\vec{\lambda})\,\mathcal{L}(x_a|\vec{\lambda})}{p(x_a)}; \quad (2)$$

in the previous Equation

$$\mathcal{L}(x_a|\vec{\lambda}) \propto \exp\left\{-2\int_{f_l}^{f_h} \frac{\left|\tilde{x}_a(f) - \tilde{h}_a(f; \vec{\lambda})\right|^2}{S_a(f)}\,df\right\} \quad (3)$$

is the *likelihood function* of the data given the model, which measures the fit of the data to the model, and $p(x_a)$ is the *marginal likelihood* or *evidence*; $\tilde{x}(f)$ stands for the Fourier component of $x(t)$. For multi-detector observations involving a network of detectors with uncorrelated noise — this is the case of this paper, where we do not use the pair of co-located LIGO instruments — we have $p(\vec{\lambda}|\{x_a; a = 1, \ldots, n_{\text{det}}\}) = \prod_{a=1}^{n_{\text{det}}} p(\vec{\lambda}|x_a)$.

The numerical computation of the joint and *marginalised* PDFs involves the evaluation of integrals over a large number of dimensions. Markov-chain Monte-Carlo (MCMC) methods (*e.g.* Gilks et al. 1996; Gelman et al. 1997, and references therein) have proved to be particularly effective in tackling

these numerical problems. We have developed an adaptive (see Figueiredo & Jain, 2002; Atchade & Rosenthal 2003) MCMC algorithm, intended to explore the parameter space efficiently while requiring the least amount of tuning for the specific signal at hand; the code is an extension of the one developed by some of the authors to explore MCMC methods for non-spinning binaries (Röver et al. 2006, 2007) and takes advantage of techniques explored by some of us in the context of LISA data analysis (Stroeer et al. 2007). A summary of the methods used in our MCMC code has been published (Van der Sluys et al. 2008); more technical details will be provided elsewhere.

Here we present results obtained by adding a signal in simulated initial-LIGO noise and computing the posterior PDFs with MCMC techniques for a fiducial source consisting of a $10\,M_\odot$ spinning BH and a $1.4\,M_\odot$ non-spinning NS in a binary system with a signal-to-noise ratio (SNR) of 17.0 for the network of 2 or 3 detectors (obtained by scaling the distance). We consider a number of cases for which we change the BH spin magnitude ($a_{\text{spin}} = 0.0, 0.1, 0.5, 0.8$) and the angle between the spin and the orbital angular momentum ($\theta_{\text{SL}} = 20°, 55°$); the remaining ten parameters, including source position and orientation of the total angular momentum, are kept constant ($\text{R.A.} = 14.3h$, Dec. $= 12°$, $\theta_{J_0} = 4°$ and $\phi_{J_0} = 289°$ for this study). For each of the seven ($a_{\text{spin}}, \theta_{\text{SL}}$) combinations (six for finite spin, one for zero spin), we run the analysis using the data from (i) the 4-km LIGO detector at Hanford (H1) and the Virgo detector near Pisa ($n_{\text{det}} = 2$), and (ii) the two LIGO 4-km interferometers (H1 and L1) and the Virgo detector ($n_{\text{det}} = 3$). This results in a total of 14 signal cases explored in this study. The MCMC analysis that we carry out on each data set consists of 5 separate serial chains, each with a length of 3.5×10^6 iterations ($n_{\text{det}} = 2$) or 2.5×10^6 iterations ($n_{\text{det}} = 3$), sampled after a *burn-in* period (see *e.g.* Gilks et al. 1996) that is determined automatically as follows: we determine the absolute maximum likelihood L_{max} that is obtained in any of the five chains, and for each chain include all the iterations *after* the chain has reached a likelihood value of $L_{\text{max}} - 2$. Each chain starts at offset (*i.e.*, non-true) parameter values. The starting values for chirp mass and the time of coalescence are drawn from a Gaussian distribution centred on the true parameter value, with a standard deviation of about $0.1\,M_\odot$ and 30 ms respectively. The other ten parameters are drawn randomly from the allowed ranges. Multiple chains starting from offset parameters and locking on to the same values for the parameters and likelihood provide convincing evidence of convergence in a blind analysis. Our MCMC code needs to run for typically one week to show the first results and 10–14 days to accumulate a sufficient number of iterations for good statistics, each serial chain using a single 2.8 GHz CPU. An example of the PDFs obtained for a signal characterised by $a_{\text{spin}} = 0.1$ and $\theta_{\text{SL}} = 20°$ is shown in panels c–f of Fig. 1, for the cases of 2 and 3 detectors; the PDFs for M_1 and M_2 in Fig. 1d are constructed from those obtained for $\mathcal{M}$ and η.

In order to evaluate the parameter-estimation accuracy we compute probability intervals; in Table 1 we report the 90%-probability interval for each of the parameters, defined as the smallest range for which the posterior probability of a given parameter to be in that range is 0.9. For the two-dimensional cases (position and orientation) we quote the smallest *area* that contains 90% of the probability. From the 140 marginalised PDFs considered here (ignoring the derived parameters M_1, M_2 and combining R.A., Dec as position and
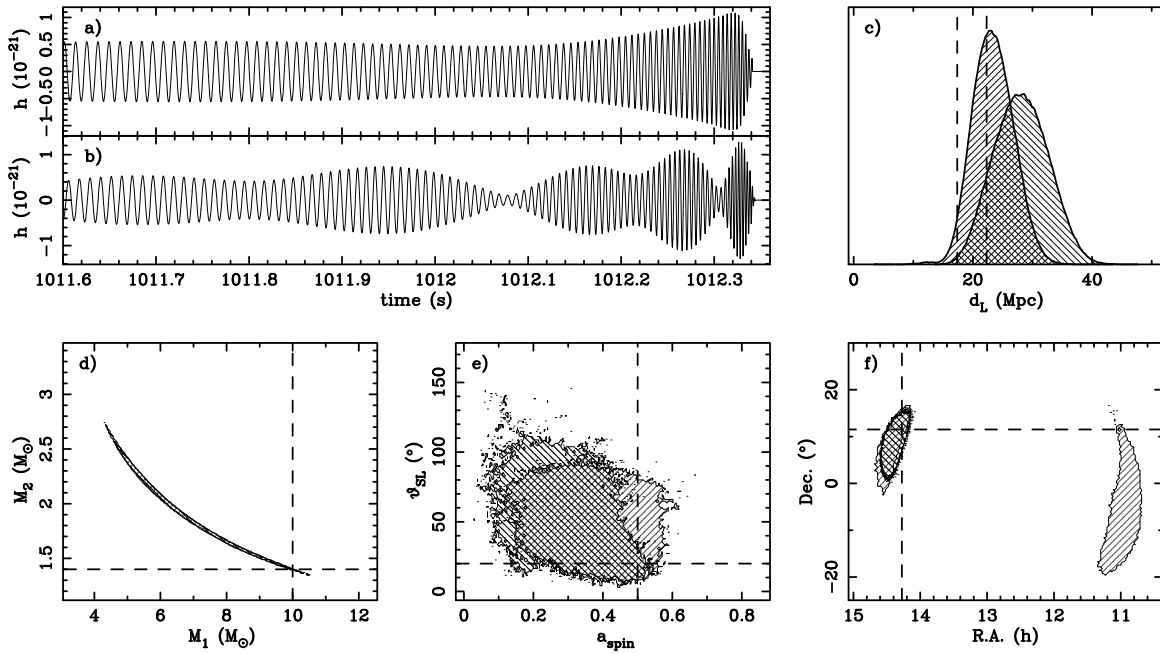
FIG. 1.— **(a)** Part of the waveform from a source with $a_{\rm spin} = 0.1$ and $\theta_{\rm SL} = 20°$. **(b)** the same waveform, but for $a_{\rm spin} = 0.8$. **(c)** Posterior PDF of the luminosity distance for a signal with $a_{\rm spin} = 0.5$ and $\theta_{\rm SL} = 20°$, as determined with the signal of two (left PDF) and three (right PDF) detectors. The dashed lines show the true distance, which is higher for the three-detector case to obtain the same SNR. **(d–f)** Two-dimensional posterior PDF showing the 99%-probability areas for the same runs as (c), for the individual masses, where the ellipses are aligned with the line of constant $\mathcal{M}$ (d), the spin parameters (e) and the position in the sky (f). The dashed lines display the true parameter values. Upward and downward hashes show the result for two and three detectors respectively in panels **(c–f)**.

$\theta_{\rm J0}$, $\phi_{\rm J0}$ as orientation), the true parameter values lie outside the 90% probability range in 27 cases, marked with superscripts in Table 1. For the 21 cases marked with [a] the true parameter is within the 99%-probability range, the 6 cases marked with [b] lie outside the 99% but inside the 100% range.

We find that most of these outliers are caused by a degeneracy between the mass and spin parameters. A parameter set with different values for $\mathcal{M}$, η, $a_{\rm spin}$ and $\theta_{\rm SL}$ can produce a waveform that is almost identical to the signal we injected. For the chirp mass and spin parameters, the distance between the two degenerate regions is relatively small. However, for the mass ratio η, these two regions ($\eta \approx 0.11$, the injected value and $\eta \approx 0.2$) are far apart and seem disconnected. A comparison of waveforms from the two degenerate regions demonstrates that their overlap is so high (match $> 99.5\%$) that it would be impossible to tell which is the true signal even at high SNR. This degeneracy could be physical or could be caused by the simplified waveform model; further investigation is warranted.

For a detection with two interferometers, the sky position and binary orientation are degenerate; for low spin, our PDFs show an incomplete ring in the sky where the source might be. When the BH spin increases, the allowed sky location shrinks appreciably until mere arcs are left (Fig. 1f). For intermediate and high spin, and $\theta_{\rm SL} = 55°$, we typically find only one such arc, reducing the sky position to several degrees (Table 1).

Even with two detectors the source parameters can be measured at astrophysically interesting levels when sufficient spin is present, including distance, individual masses, spin magnitude and tilt angle; for $a_{\rm spin} = 0.5$ or more, the typical uncertainty in the sky position is a few tens of square degrees, the distance is determined with 20–60% accuracy and the timing accuracy is 6 ms or better.

The accuracy of the parameter determination is affected by the number of detectors used, a result well established in studies of inspirals of non-spinning compact objects (*e.g.* Jara-

nowski, P., & Krolak 1994; Pai et al. 2001; Cavalier et al. 2006; Röver et al. 2007). Unlike some other studies, we keep the SNR of the detector network constant; when a third detector is added, the distance to the source is increased (Fig. 1c). This way, we see the effect of the additional information that is provided by the extra interferometer and eliminate the effect of the higher SNR. Table 1 shows that the effect on the uncertainty in the mass and spin parameters is marginal when adding a third interferometer to the network. The uncertainty in the distance and time of coalescence decreases typically by 20–25% when using three detectors, but the largest effect is on the accuracy for sky position and binary orientation; Table 1 shows that the (two-dimensional) uncertainties in these parameters decrease by 50% and 40% respectively on average.

The parameter-estimation accuracy also depends strongly on the actual spin parameters of the system: as a general trend, the larger $a_{\rm spin}$ and $\theta_{\rm SL}$, the stronger the modulations in the waveform induced by precession, and the more information is coded up in the waveform. When we divide our simulations into low spin ($a_{\rm spin} = 0.0, 0.1$) and high spin ($a_{\rm spin} = 0.5, 0.8$) cases, we find that the uncertainties in the high-spin case are smaller by 40–60% for the masses, time of coalescence and distance, by 65–70% for the spin parameters and by 80–90% for the sky position and binary orientation. However, the width of the 90%-probability interval is in fact not strictly monotonic as a function of $a_{\rm spin}$ and $\theta_{\rm SL}$ (Table 1). The increasingly complex structure of the likelihood function and stronger correlations amongst different parameters for higher spin have an important effect on the sampling efficiency of the MCMC.

Earlier studies (*e.g.* Cutler & Flanagan (1994, their Tables II & III and Fig. 7); Poisson & Will (1995, their Table II); Van den Broeck & Sengupta (2007, their Table III)) have reported on the theoretical accuracy of parameter estimation. These explorations are based on the Fisher matrix, which

4 M.V. van der Sluys et al.

TABLE 1
INJECTION DETAILS AND WIDTHS OF THE 90%-PROBABILITY INTERVALS OF THE MCMC RUNS DESCRIBED IN THE TEXT

$n_{\rm det}$	$a_{\rm spin}$	$\theta_{\rm SL}$ (°)	$d_{\rm L}$ (Mpc)	M_1 (%)	M_2 (%)	$\mathcal{M}$ (%)	η (%)	$t_{\rm c}$ (ms)	$d_{\rm L}$ (%)	$a_{\rm spin}$	$\theta_{\rm SL}$ (°)	$\phi_{\rm c}$ (°)	$\alpha_{\rm c}$ (°)	Pos. (°²)	Ori. (°²)
2	0.0	0	16.0	95	83	2.6	138	18	86	0.63	—	323	—	537	19095
2	0.1	20	16.4	102	85	1.2	90	10	91	0.91	169	324	326^a	406	16653
2	0.1	55	16.7	51	38	0.88	59	7.9	58	0.32	115	322	326	212	3749
2	0.5	20	17.4	53^b	42^a	0.90	50^b	5.4	46^a	0.26	56	330	301^b	111^a	3467^a
2	0.5	55	17.3	31	24	0.62	41	4.9	21	0.12	24	323	269^a	19.8	178^a
2	0.8	20	17.9	54^a	42^a	0.86^a	54^a	6.0	56	0.16	25^a	325	319	104^a	1540
2	0.8	55	17.9	21	16	0.66	29	4.7	22	0.15	15	320	323	22.8	182^a
3	0.0	0	20.5	114	90	2.6	119	15	69	0.98^b	—	325	—	116	4827
3	0.1	20	21.1	70	57	0.92	72	7.0	60	0.49	160	321	322^a	64.7	3917
3	0.1	55	21.4	62	48	0.93	68	6.2	51	0.52	123	325	308^a	48.7	976
3	0.5	20	22.3	54^b	44^a	0.89^a	48^b	3.3	52	0.28^a	69	318	229^b	28.8	849
3	0.5	55	22.0	33	25	0.62	43	4.6	23^a	0.14	27	322	324	20.7	234^a
3	0.8	20	23.0	53^b	41^a	0.85^a	52^b	3.8	55	0.17	23^a	320	327^a	36.4^a	645
3	0.8	55	22.4	30	22	0.86	40	5.0	26	0.21	21	322	323	27.2	288

^{a} the true value lies outside the 90%-probability range; ^{b} idem, outside the 99%-probability range, but inside the 100% range

yields the expected uncertainty (for unimodal distributions), without actually estimating the parameter values themselves. The quoted accuracies for masses and the time and phase of coalescence are typically better than or similar to the values in our Table 1. We have been able to estimate distance, sky position and binary orientation to better accuracy than suggested in these studies.

4. CONCLUSIONS

We have explored for the first time the parameter estimation of all physical parameters — including masses, spin, distance, sky location and binary orientation — on ground-based gravitational-wave observations of binary inspirals with spinning compact objects. We show that for two detectors and sufficient spin ($a_{\rm spin} \geq 0.5$) or for three detectors, the obtained accuracy in sky position, distance and time of coalescence is good enough to allow the identification of electromagnetic counterparts of compact-binary mergers, *e.g.* short gamma-ray bursts (Nakar 2007). A direct measurement of mass, spin, distance and orientation can be obtained from inspiral GWs, which is notoriously difficult for electromagnetic observations.

The analysis presented here is the first step of a more detailed study that we are currently carrying out, exploring a much larger parameter space, developing techniques to reduce the computational cost of these simulations, and testing the methods with actual LIGO data. The waveform model used here, though adequate for exploratory studies, is not sufficiently accurate for the analysis of real detections, and we are finalising the implementation of a more realistic waveform. Simulations with this improved waveform may also shed light on the degeneracy between mass and spin parameters discussed in Sect. 3, and may improve the accuracy of our parameter estimation appreciably (*e.g.* Van den Broeck & Sengupta 2007). Finally, we intend to further develop our Bayesian approach into one of the standard tools that can be included in the analysis pipeline used for the processing of the 'science data' collected by ground-based laser interferometers.

REFERENCES

Apostolatos, T. A., Cutler, C., Sussman, G. J., & Thorne, K. S. 1994, Phys. Rev. D, 49, 6274
Arcese, F., et al. 2004, Class. Quant. Grav., 21, 385
Atchade, Y. F., & Rosenthal, J. S. 2005, Bernoulli 11(5) 815
Barish, B. C., & Weiss, R. 1999, Physics Today, 52, 44
Blanchet, L., Damour, T., Iyer, B. R., Will, C. M., & Wiseman, A. G. 1995, Phys. Rev. Lett., 74, 3515
Blanchet, L., Buonanno, A., & Faye, G. 2006, Phys. Rev. D, 74, 104034
Buonanno, A., Chen, Y., & Vallisneri, M. 2003, Phys. Rev. D, 67, 104025. Erratum-ibid. 2006, 74, 029904(E)
Cavalier, F., et al. 2006, Phys. Rev. D, 74, 082004
Cutler, C. & Flanagan, E. E. 1994, Phys. Rev. D, 49, 2658
Cutler, C. and Thorne, K. S., 2002, gr-qc/0204090
Faye, G., Blanchet, L., & Buonanno, A. 2006, Phys. Rev. D, 74, 104033
Figueiredo, M. A. T., & Jain, A. K. 2002, IEEE Transactions on Pattern Analysis and Machine Intelligence, 24, 281
Gelman, A., Carlin, J. B., Stern, H., & Rubin, D. B. 1997, *Bayesian data analysis*, Chapman & Hall, Boca Raton
Gilks, W. R., Richardson, S., & Spiegelhalter, D. J. 1996, *Markov chain Monte Carlo in practice*, Chapman & Hall

Grandclément, P., Kalogera, V., & Vecchio, A. 2003, Phys. Rev. D, 67, 042003
Jaranowski, P., & Krolak, A. 1994, Phys. Rev. D, 49, 1723
Kidder, L. E. 1995, Phys. Rev. D, 52, 821
Lang, R. N., & Hughes, S. A. 2006, Phys. Rev. D, 74, 122001. Erratum-ibid. 2007, 75, 089902(E)
Nakar, E. 2007, Phys. Rep., 442, 166
O'Shaughnessy, R., Kalogera, V., & Belczynski, K. 2008, ApJ, 672, 479
Pai, A., Dhurandhar, S., & Bose, S. 2001, Phys. Rev. D, 64, 042004
Poisson, E. & Will, C. M. 1995, Phys. Rev. D, 52, 848
Röver, C., Meyer, R., & Christensen, N. 2006, Class. Quant. Grav., 23, 4895
Röver, C., Meyer, R., & Christensen, N. 2007, Phys. Rev. D, 75, 062004
Stroeer, A., et al. 2007, Class. Quant. Grav., 24, 541
Takahashi, R., & the TAMA Collaboration 2004, Class. Quant. Grav., 21, 403
Van den Broeck, C. & Sengupta, A. S. 2007, Class. Quant. Grav. 24, 1089
Van der Sluys, M., et al. 2008, Class. Quant. Grav., in press, arXiv:0805.1689
Vecchio, A. 2004, Phys. Rev. D, 70, 042001
Willke, B., et al. 2004, Class. Quant. Grav., 21, 417